

# Diffusion-weighted imaging and pathology of chronic kidney disease: initial study

Xueqin Xu,<sup>1</sup> Suzanne L. Palmer,<sup>2</sup> Xiaozhu Lin,<sup>1</sup> Weixia Li,<sup>1</sup> Kemin Chen,<sup>1</sup> Fuhua Yan,<sup>1</sup> Xiao Li<sup>3</sup>

<sup>1</sup>Department of Radiology, Shanghai Jiao Tong University Medical School Affiliated Ruijin Hospital, Shanghai, China

<sup>2</sup>Clinical Radiology and Medicine, Keck Medical Center, University of Southern California, Los Angeles, CA, USA

<sup>3</sup>Department of Nephrology, Shanghai Jiao Tong University Medical School Affiliated Ruijin Hospital, No. 197, Ruijin ER Road, Shanghai 200025, China

## Abstract

**Purpose:** To investigate the value of diffusion-weighted imaging (DWI) for assessing histopathologic changes observed in chronic kidney disease (CKD).

**Methods:** Fifty-two patients with CKD underwent DWI before renal biopsy. The renal apparent diffusion coefficient (ADC) values and histopathologic changes were analyzed. The pathologic changes were scored using a semi-quantitative method (no lesion as 0, mild lesion as 1, moderate lesion as 2, and severe lesion as 3). The relationships between renal histopathologic scores, types, classification, and right renal ADCs were analyzed using ANOVA and Pearson's or Spearman's correlation tests.

**Results:** Negative correlations were found between the right renal ADCs and scores of tubulointerstitial lesions ( $r = -0.354$ ,  $P = 0.012$ ), the severity of tubular atrophy ( $r = -0.439$ ,  $P = 0.002$ ), and the severity of interstitial fibrosis ( $r = -0.272$ ,  $P = 0.049$ ). There were no correlations between the ADCs and scores of glomeruli and peritubular vessel lesions ( $P > 0.05$ ). There were significant differences among groups based on pathology types ( $P = 0.009$ ). There was no significant relationship between renal ADCs and the pathologic classification ( $P > 0.05$ ).

**Conclusions:** DWI may be helpful to detect tubulointerstitial injury, including tubular atrophy and interstitial fibrosis. DWI may have the potential to serve as an effective auxiliary method to help nephrologists to evaluate patients with CKD.

**Key words:** Chronic kidney disease—Magnetic resonance imaging—Diffusion-weighted imaging—Apparent diffusion coefficient—Pathologic changes

As a significant public health problem, chronic kidney disease (CKD) is increasing in the United States and worldwide [1]. Patients with end-stage renal disease (ESRD) are confronted with high costs and poor outcomes [2]. Because the progression of CKD is often slow and lacks specific symptoms [1], identification of renal pathology (type and severity) is essential for planning the treatment and prediction of long-term outcomes of renal function in CKD [3]. Renal biopsy is the most useful and readily available technique to identify the renal pathology in CKD [4], but the risks of renal biopsy, such as hematuria, perirenal hematoma, and infection, make it a less desirable method for follow-up [5]. Non-invasive, quantitative markers for CKD are needed to reduce the dependence on percutaneous biopsies and to identify those patients who would benefit most from percutaneous renal biopsy.

Diffusion-weighted imaging (DWI) is one such potential quantitative method that has shown great potential for research and clinical applications [6]. Because DWI can provide several parameters that describe the restriction of the Brownian random motion of water molecules in biologic tissues [6], DWI had previously been used in the assessment of renal function in previous studies [7–9]. Recent experimental models and clinical studies found a relationship between DWI and renal fibrosis [10–12]; however, diagnosis of specific renal pathology in CKD requires more than identifying renal fibrosis. Renal pathology includes the identification of impairments of renal glomeruli, tubules, and blood ves-

sels [13]. Tailoring patient therapy and follow-up is achieved by identifying specific renal pathology and not just the presence of fibrosis, the final common pathway.

The objective of our study was to evaluate the value of DWI as a quantitative method for different renal pathology for the assessment of patients with a clinical diagnosis of CKD.

## Methods

### *Study population*

Fifty-two patients (29 men, 23 women; mean age, 36 years; age range 18–62 years) were successfully included from October 1, 2011 to December 31, 2012. Patients were included if they met the following criteria: (a) met clinical diagnostic criteria for CKD; (b) had renal pathology by renal biopsy; (c) had no other medical diagnosis that may affect renal function, such as gout, diabetes, or hypertension; and (d) had magnetic resonance imaging (MRI) with DWI 2–10 days prior to renal biopsy. Patients were excluded if they exhibited any of the following: (a) they could not tolerate MRI examination; (b) the image quality did not meet requirements of the study; (c) there were malignant or multiple benign renal masses that could affect data analysis; or (d) if renal biopsy could not be performed. Eight patients were excluded because of these exclusion criteria.

This study was approved by the institutional ethics committee, and each subject provided written informed consent prior to enrollment.

### *MRI protocol*

The following pulse sequences were performed: (1) coronal T2-weighted single-shot fast spin-echo [5 mm section thickness, 1 mm gap, 6316/102 ms (repetition time/echo time), 380 × 380-mm field of view (FOV), 320 × 224 matrix, half-Fourier acquisition, 1.2 × 1.7 × 5.0 mm voxel]; twenty sections were acquired, with a total acquisition time, 2 min 22 s; (2) coronal T1-weighted fast spoiled gradient-echo [5 mm section thickness, 1 mm gap, 380 × 380-mm FOV, 320 × 192 matrix, one signal acquired, 210/1.5 ms (repetition time/echo time), 80° flip angle, 50-kHz bandwidth, NEX 1; number of sections acquired, 20; acquisition time, 20 s]; (3) coronal DW multisection echo-planar MR with b values of 0 and 500 s/mm<sup>2</sup> [2000/52.9 ms (repetition time/echo time), 5 mm section thickness, 1 mm gap, 256 × 256 matrix, 380 × 380-mm FOV, 250-kHz bandwidth, NEX 2]. Fat saturation was used to avoid chemical shift artifacts. The diffusion gradients were applied in three orthogonal directions and subsequently averaged to minimize the effects of diffusion anisotropy. The entire sequence consisted of 11 sections, with a single breath hold, 16-second acquisition time.

A 1.5-T MR imager (GE Signa Excite HD Twin-Speed 1.5T, General Electric Medical Systems, Milwaukee, WI) with 40 mT/m maximum gradient capability and an eight-channel body coil (General Electric Medical Systems, Milwaukee, WI) was used.

### *Image analysis*

Image analysis was performed at a GE workstation (Sun Microsystems, ADW4.2, General Electric Medical Systems, Milwaukee, WI) with Functool 2 image analysis software (GE Medical Systems, Milwaukee, WI, USA). Evaluation of images was performed by 2 radiologists experienced in abdominal imaging (X.X., 16 years and F.Y., 27 years). Using the coronal apparent diffusion coefficient (ADC) map, freehand regions of interest (ROIs) were positioned in the parenchyma to include the cortex and medullary pyramids (Fig. 1). Then, ADC values of the freehand ROIs were calculated. Because the ultrasound-guided biopsies were completed in the right kidney, the right renal ADC values were used for analysis.

### *Renal biopsy*

Ultrasound-guided, core biopsies were performed by a nephrologist experienced in percutaneous renal biopsy (X.L., 24 years). Patients were placed prone on the examination table after urination. The inferior pole of the right kidney was selected as the biopsy site in all

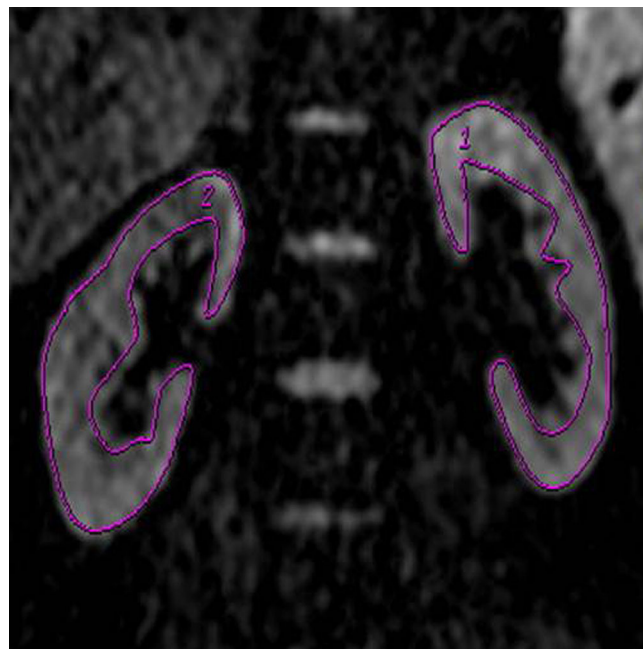


**Fig. 1.** The measurement approaches. The ROIs of kidneys were drawn freehand in the entire parenchyma of the renal mesorenal area.

**Table 1.** CKD patient pathology type, age, gender

Pathological type	Cases (n) (male/female)	Age (years)
Focal segmental glomerulosclerosis (FSGS)	12 (9 M/3 F)	20–59
IgA nephropathy (IgAN)	23 (11 M/12 F)	20–62
Minimal change nephropathy (MCN)	5 (4 M/1 F)	18–33
IgM nephropathy	1 (1 F)	50
Lupus nephritis	1 (1 F)	32
Mesangial proliferative glomerulonephritis	4 (2 M/2 F)	21–52
Membranous nephropathy	1 (1 M)	34
Renal amyloidosis	1 (1 F)	53
Sclerosing glomerulonephritis	2 (2 M)	28–52
Crescentic glomerulonephritis	1 (1 M)	27
Diffuse endocapillary proliferative glomerulonephritis with crescent formation	1 (1 F)	20

CKD, chronic kidney disease; n, number of patients

**Table 2.** Relationship between right renal ADCs and renal histopathologic scores

Analysis	Glomerular score	Glomerulosclerosis score	Tubulointerstitial score	Intrarenal arterial score
Pearson				
<i>r</i>	– 0.237	– 0.155	– 0.354	– 0.272
<i>p</i>	0.104	0.254	<b>0.012</b>	0.062

Bold value indicates statistical significance ( $P < 0.05$ )

ADC, apparent diffusion coefficient

patients. The specimen was deemed adequate for histopathology examination when the renal tissue specimen contained more than six glomeruli.

### Renal histopathologic analysis

Renal histopathologic examination and analysis was performed by a pathologist with more than 20 years of experience in renal disease. Pathology types were classified according to the 2012 Kidney Disease Improving Global Outcomes (KDIGO) [14]. Because IgA nephropathy (IgAN), a common form of CKD, accounted for a large proportion of cases in our study, patients with IgAN were classed by the Haas classification [15] to analyze the relationship between DWI and the pathologic classification.

The glomerular, tubulointerstitial, and intrarenal arterial lesion involvement were scored using a semi-quantitative method: no lesion = 0, mild lesion ( $\leq 25\%$ ) = 1, moderate lesion (25%–50%) = 2, and severe lesion ( $\geq 50\%$ ) = 3. The tubulointerstitial score included assessments of tubular atrophy, interstitial fibrosis, and interstitial inflammatory cell infiltration. The glomerular score included assessments of mesangial proliferation, mesangial matrix increase, and glomerulosclerosis. The intrarenal arterial score included assessments of myointimal hyperplasia, microthrombosis, and arteriosclerosis.

### Statistical analysis

Statistical analysis was performed using the SPSS 19.0 analyze software package. The ADC values of patients

with CKD were reported as the mean  $\pm$  standard deviation. The relationship between the right renal ADCs and renal histopathologic scores was analyzed using Pearson's correlation test. Spearman's correlation tests were used to analyze the relationship between right renal ADC values and the degree of tubular atrophy and between ADCs and the degree of interstitial fibrosis. ANOVA and Spearman's correlation tests were used to analyze the differences of ADCs among pathologic types and the relationship between ADCs and the IgAN pathologic classification, respectively. A  $P$  value less than 0.05 was considered a statistically significant difference.

## Results

### Pathologic results

Renal core biopsies and histopathologic examinations were completed successfully in 52 patients. The pathologic results of all patients are listed in Table 1.

### Relationship between ADC and histopathologic changes

A negative correlation was found between the renal ADCs and scores of tubulointerstitial lesions ( $r = -0.354$ ,  $P = 0.012$ ). However, there were no correlations between the renal ADCs and scores of other pathologic changes, including glomerular and intrarenal arterial lesions ( $P > 0.05$ ) (Table 2).

Spearman's correlation analysis revealed a significant negative correlation between the ADC value of renal parenchyma and severity of tubular atrophy ( $r = -0.439$ ,  $P = 0.002$ ) (Figs. 2, 3, 4 and 5). There was a



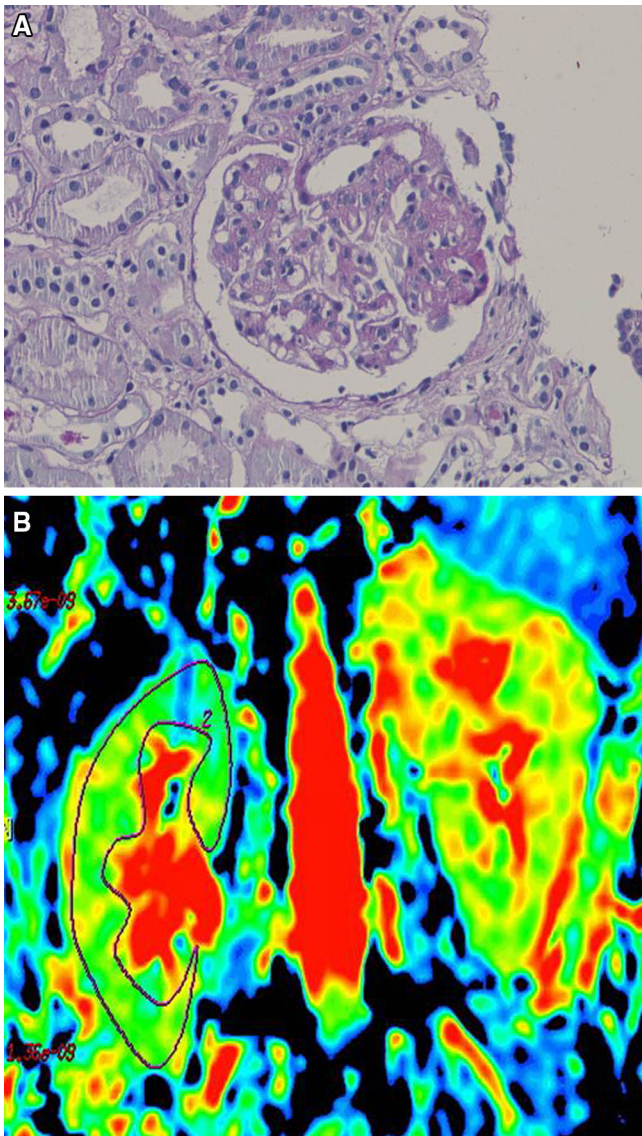


Fig. 2. Renal micrograph (A) and ADC map (B) in a 32-year-old female with no tubular atrophy. No tubular atrophy and moderate mesangial proliferation are shown in the right renal micrograph (A) (periodic acid-Schiff (PAS) stain,  $\times 200$ ). The ADC value of the right kidney was  $2.45 \times 10^{-3} \text{ mm}^2/\text{s}$  (B).

significant difference in ADCs among patients with varying degrees of tubular atrophy ( $F = 5.967$ ,  $P = 0.002$ ). The ADCs were significantly lower in patients with severe tubular atrophy than in those with no tubular atrophy ( $P = 0.000$ ), mild tubular atrophy ( $P = 0.001$ ), or moderate tubular atrophy ( $P = 0.035$ ). However, no significant differences were found in ADCs among patients with no, mild or moderate tubular atrophy (Table 3). There was a mild negative correlation between renal ADCs and the severity of interstitial fibrosis ( $r = -0.272$ ,  $P = 0.049$ ). No significant differences were found in ADCs among patients with no,

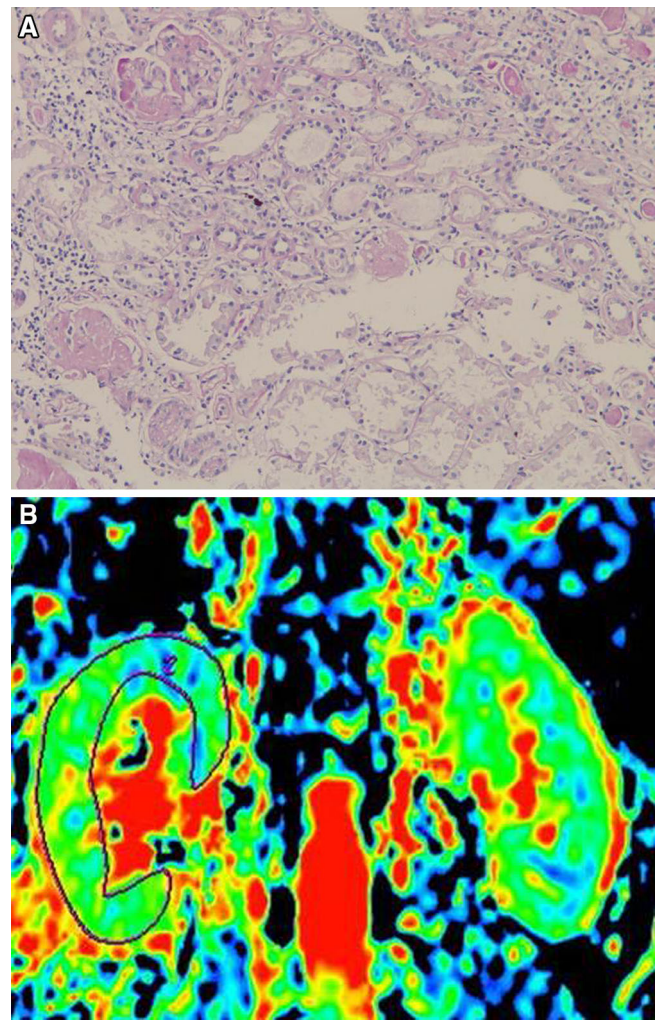


Fig. 3. Renal micrograph (A) and ADC map (B) in a 40-year-old male with mild tubular atrophy. Mild tubular atrophy, interstitial infiltration of lymphocytes and glomerulosclerosis are shown in the right renal micrograph (A) (periodic acid-Schiff (PAS) stain,  $\times 100$ ). The ADC value of the right kidney was  $2.40 \times 10^{-3} \text{ mm}^2/\text{s}$  (B).

mild, moderate, or severe renal interstitial fibrosis ( $F = 2.169$ ,  $P = 0.104$ ).

#### *Relationship between ADC and pathologic types*

To differentiate CKD pathology types, the analysis of renal ADC values showed there were significant differences among groups based on pathology types ( $F = 5.322$ ,  $P = 0.009$ ). Patients with minimal change nephropathy (MCN) had higher renal ADCs ( $2.66 \pm 0.12 \times 10^{-3} \text{ mm}^2/\text{s}$ ) than those with IgAN ( $2.40 \pm 0.16 \times 10^{-3} \text{ mm}^2/\text{s}$ ) ( $P = 0.012$ ) and focal segmental glomerulosclerosis (FSGS) ( $2.33 \pm 0.25 \times 10^{-3} \text{ mm}^2/\text{s}$ ) ( $P = 0.011$ ). However, there was no significant difference in ADCs between patients with IgAN and FSGS ( $P = 0.835$ ).



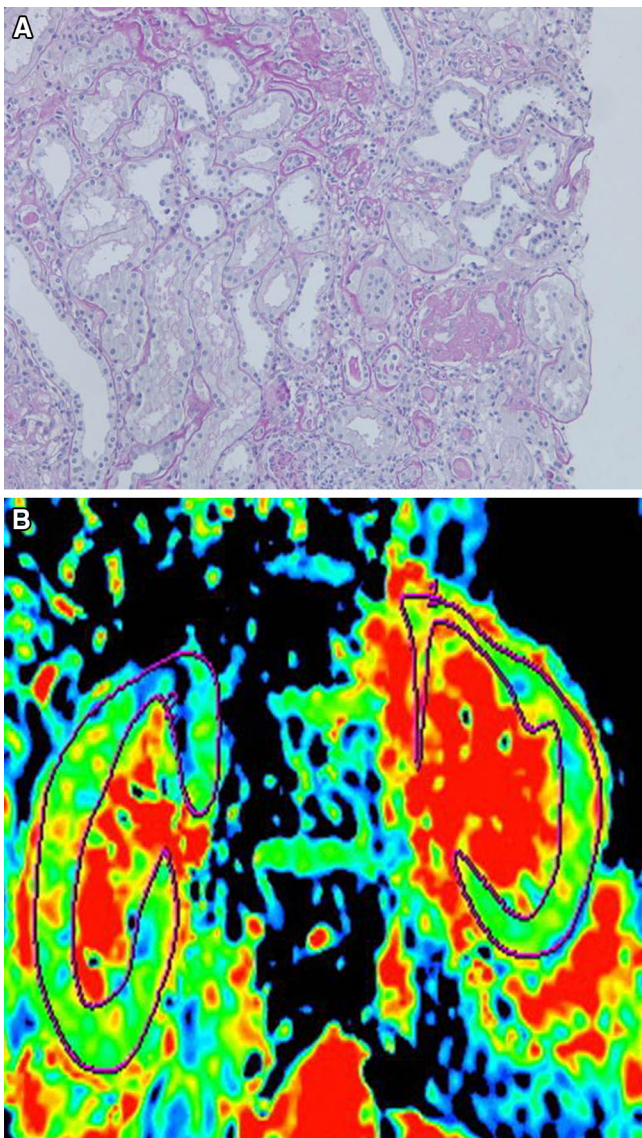


**Fig. 4.** Renal micrograph (A) and ADC map (B) in a 47-year-old male with moderate tubular atrophy. Moderate tubular atrophy, interstitial infiltration of lymphocytes, and glomerulosclerosis are shown in the right renal micrograph (A) (periodic acid-Schiff (PAS) stain,  $\times 100$ ). The ADC value of the right kidney was  $2.34 \times 10^{-3} \text{ mm}^2/\text{s}$  (B).

#### *Relationship between ADC and pathologic classification*

Among the different Haas classifications in IgAN, there was no significant relationship between renal ADCs and the pathologic classification ( $r = -0.367$ ,  $P = 0.102$ ). Although the renal ADCs were higher in IgAHAasII, there was no significant difference in renal ADC values among the different Haas classifications for IgAN ( $F = 1.425$ ,  $P = 0.270$ ).

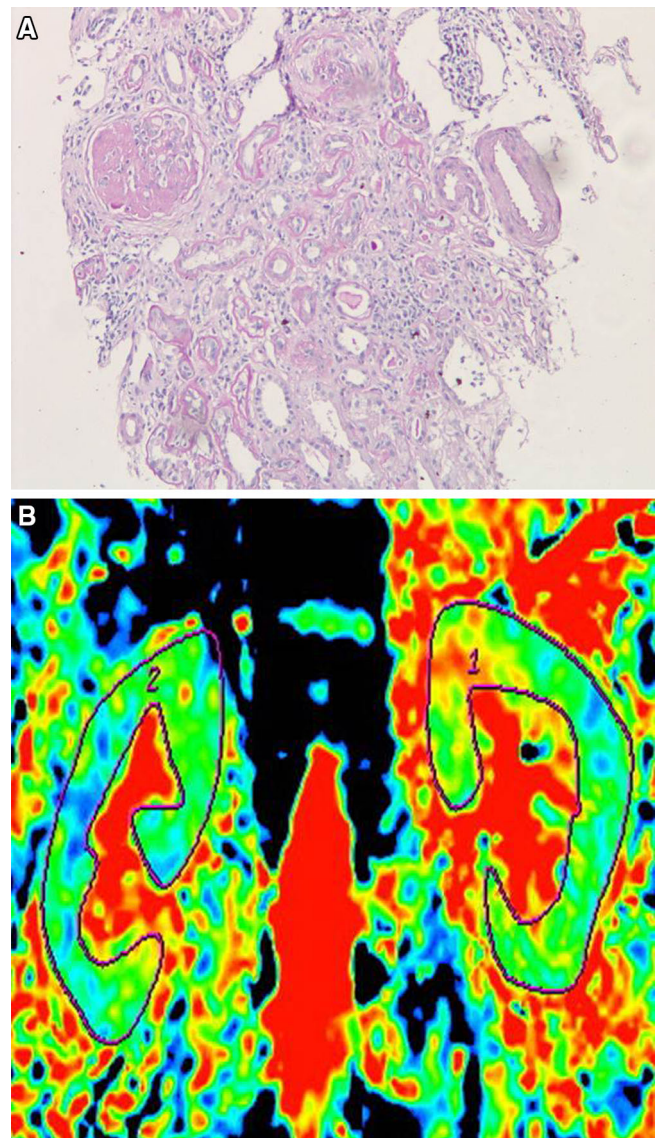


**Fig. 5.** Renal micrograph (A) and ADC map (B) in a 42-year-old male with severe tubular atrophy. Severe tubular atrophy, severe interstitial fibrosis with infiltration of lymphocytes and glomerulosclerosis are shown in the right renal micrograph (A) (periodic acid-Schiff (PAS) stain,  $\times 100$ ). The ADC value of the right kidney was  $2.18 \times 10^{-3} \text{ mm}^2/\text{s}$  (B).

**Table 3.** Renal ADC value in patients with various severity of tubular atrophy

Severity of tubular atrophy	Cases (n)	ADC of right kidney ( $\times 10^{-3} \text{ mm}^2/\text{s}$ )
No tubular atrophy	9	$2.51 \pm 0.31$
Mild tubular atrophy	22	$2.44 \pm 0.23$
Moderate tubular atrophy	12	$2.33 \pm 0.20$
Severe tubular atrophy	9	$2.10 \pm 0.12$

Data are mean  $\pm$  standard deviation; n, number of cases; ADC, apparent diffusion coefficient

## Discussion

CKD is characterized by the progressive loss of kidney function due to tubular atrophy, interstitial fibrosis, glomerular scarring, and a reduction of blood flow [11]. Tubulointerstitial lesion is a final common pathway for progressive renal injury in most glomerulopathies, and the level of tubulointerstitial fibrosis correlates closely with the degree of chronic renal dysfunction [16–18]. Clinically, information about tubulointerstitial lesions in patients with CKD was acquired by renal biopsy. We applied a non-invasive method (DWI) to investigate the relationship between ADC values and specific renal pathology in CKD. Theoretically, any pathological changes of renal tissues would influence perfusion and diffusion in the extracellular extravascular space and affect the ADC values of renal parenchyma [19].

In the present study, a negative correlation was observed between renal ADCs and tubulointerstitial lesions ( $r = -0.354$ ), whereas no significant correlation was found between renal ADCs and glomerular or intrarenal arterial lesions. These findings suggest that tubulointerstitial lesions have greater influence on the random motion of water in the extravascular extracellular space and cause a decrease in ADC. Li et al. [20] also found that renal DWI was closely associated with renal tubulointerstitial lesions.

In addition, we also found negative relationships between renal ADCs and the severity of tubular atrophy ( $r = -0.439$ ) and ADCs and the severity of interstitial fibrosis ( $r = -0.272$ ). Renal ADCs had a higher correlation with the degree of tubular atrophy ( $r = -0.439$ ) than with tubulointerstitial lesion scores ( $r = -0.354$ ). There was a mild negative correlation between renal ADCs and the severity of interstitial fibrosis ( $r = -0.272$ ). No significant differences were found in ADCs among patients with no, mild, moderate or severe renal interstitial fibrosis. These results suggest that renal tubular lesions have greater influence on the progress of CKD, and diffusion in the extracellular extravascular space, and reducing the ADC values of renal parenchyma. Furthermore, the ADC value of severe tubular atrophy was significantly lower than the other three groups (no, mild and moderate tubular atrophy). When the degree of tubular atrophy increased, the ADC values showed a gradual decline. This may be because the change of renal tubular pathology is gradual, not staged. Further research is needed to validate our findings.

For investigating the ADC value for assessing the renal pathologic type in CKD, we analyzed the renal ADCs of the most common pathological types found in our study, MCN, IgAN and FSGS. Our results showed that the ADCs of MCN were significantly higher than the other two types. Compared to the other two pathological types, the pathological change in MCN is milder, with less of an effect on both capillary perfusion and

water diffusion. Therefore, we propose that this is the cause for its higher ADC value. However, there was no difference in ADCs between IgAN and FSGS. This was different from the results of Li et al. [13] who found no significant differences in ADC values among the various pathological types. The following possible explanations may explain this finding: (1) the number of patients with different pathology types is different, and (2) the severity of pathologic change in patients may be different. Together with the literature, our results suggest that DWI changes may not be related to the specific pathological type of CKD, but instead may be related to the severity of renal pathology [13].

We found no significant relationship between renal ADCs and the different Haas classifications for IgAN. Because the Haas classifications of IgAN are primarily based on glomerular changes [21], this result indirectly suggests that there is no relationship between ADCs and renal glomerular changes.

Of course, the results of calculating the ADC are broadly variable and influenced by the type of equipment and sequence used. So, to avoid the impact of the variability of the results of the quantitative evaluation of ADC values, all patients underwent DWI in a 1.5-T MR imager with the same sequence in our study.

The renal ADCs were different with the results of Xu et al. [22] who used the same imager and b values with our study. The reason may be the different purposes of two studies. They evaluated the relationship between the ADCs and GFR, while our study investigated the value of DWI for assessing histopathologic changes in the patients with CKD. In addition, all patients were with CKD in our study, while 37 patients with renal artery stenosis and 12 patients with CKD were in their study.

There were several limitations in this study. First, the sample size was relatively small. A larger sample size is needed to analyze the generalizability of conclusions in future studies. Second, the value of ADC in assessing the prognosis and monitoring treatment is not discussed.

In conclusion, DWI, as a non-invasive functional imaging technique, may be helpful to detect tubulointerstitial injury, including tubular atrophy and interstitial fibrosis. DWI maybe has the potential to serve as an effective auxiliary method to help nephrologists evaluate patients with CKD.

### Compliance with ethical standards

**Funding** This study was funded by National Natural Science Foundation of China (81170761).

**Conflict of interest** All authors declare that they have no conflict of interest.

**Ethical approval** All procedures performed in studies involving human participants were in accordance with the ethical standards of the local ethics committee.

**Informed consent** Informed consent was obtained from all individual participants included in the study.

## References

1. Levey AS, Inker LA, Matsushita K, et al. (2014) GFR decline as an end point for clinical trials in CKD: a scientific workshop sponsored by the National Kidney Foundation and the US Food and Drug Administration. *Am J Kidney Dis* 64(6):821–835
2. Collins AJ, Foley RN, Herzog C, et al. (2013) US renal data system 2012 annual data report. *Am J Kidney Dis*. 61(1):e1–e476
3. Shiiki H, Saito T, Nishitani Y, et al. (2004) Prognosis and risk factors for idiopathic membranous nephropathy with nephrotic syndrome in Japan. *Kidney Int*. 65(4):1400–1407
4. Cagnoli L, Italian Society of Nephrology (2003) Instructions and implementations for percutaneous renal biopsy. Guidelines for the therapy of glomerular nephropathies. *G Ital Nefrol*. 20(Suppl 24):S3–47
5. Parrish AE (1992) Complications of percutaneous renal biopsy: a review of 37 years' experience. *Clin Nephrol*. 38(3):135–141
6. Ebrahimi B, Textor SC, Lerman LO (2014) Renal relevant radiology: renal functional magnetic resonance imaging. *Clin J Am Soc Nephrol*. 9(2):395–405
7. Zhang AH, Tam P, LeBlanc D, et al. (2009) Natural history of CKD stage 4 and 5 patients following referral to renal management clinic. *Int Urol Nephrol*. 41(4):977–982
8. Xu X, Fang W, Ling H, et al. (2010) Diffusion-weighted MR imaging of kidneys in patients with chronic kidney disease: initial study. *Eur Radiol*. 20(4):978–983
9. Thoeny HC, Zumstein D, Simon-Zoula S, et al. (2006) Functional evaluation of transplanted kidneys with diffusion-weighted and BOLD MR imaging: initial experience. *Radiology*. 241(3):812–821
10. Inoue T, Kozawa E, Okada H, et al. (2011) Noninvasive evaluation of kidney hypoxia and fibrosis using magnetic resonance imaging. *J Am Soc Nephrol*. 22(8):1429–1434
11. Zhao J, Wang ZJ, Liu M, et al. (2014) Assessment of renal fibrosis in chronic kidney disease using diffusion-weighted MRI. *Clin Radiol*. 69(11):1117–1122
12. Togao O, Doi S, Kuro-o M, et al. (2010) Assessment of renal fibrosis with diffusion-weighted MR imaging: study with murine model of unilateral ureteral obstruction. *Radiology* 255(3):772–780
13. Li Q, Li J, Zhang L, et al. (2014) Diffusion-weighted imaging in assessing renal pathology of chronic kidney disease: a preliminary clinical study. *Eur J Radiol*. 83(5):756–762
14. Beck L, Bomback AS, Choi MJ, et al. (2013) KDOQI US commentary on the 2012 KDIGO clinical practice guideline for glomerulonephritis. *Am J Kidney Dis*. 62(3):403–441
15. Haas M (1997) Histologic subclassification of IgA nephropathy: a clinicopathologic study of 244 cases. *Am J Kidney Dis*. 29(6):829–842
16. Thoeny HC, De Keyzer F, Oyen RH, et al. (2005) Diffusion-weighted MR imaging of kidneys in healthy volunteers and patients with parenchymal diseases: initial experience. *Radiology*. 235(3):911–917
17. Healy E, Brady HR (1998) Role of tubule epithelial cells in the pathogenesis of tubulointerstitial fibrosis induced by glomerular disease. *Curr Opin Nephrol Hypertens*. 7(5):525–530
18. Norman JT, Fine LG (2006) Intrarenal oxygenation in chronic renal failure. *Clin Exp Pharmacol Physiol*. 33(10):989–996
19. Hodgkins KS, Schnaper HW (2012) Tubulointerstitial injury and the progression of chronic kidney disease. *Pediatr Nephrol*. 27(6):901–909
20. Li X, Xu X, Zhang Q, et al. (2014) Diffusion weighted imaging and blood oxygen level-dependent MR imaging of kidneys in patients with lupus nephritis. *J Transl Med*. 12:295
21. Lee HS, Lee MS, Lee SM, et al. (2005) Histological grading of IgA nephropathy predicting renal outcome: revisiting H. S. Lee's glomerular grading system. *Nephrol Dial Transplant*. 20(2):342–348
22. Xu Y, Wang X, Jiang X (2007) Relationship between the renal apparent diffusion coefficient and glomerular filtration rate: preliminary experience. *J Magn Reson Imaging*. 26(3):678–681